Miner Deposita (2006) 41: 645–659
DOI 10.1007/s00126-006-0088-0

ARTICLE

D. Craw · M. Begbie · D. MacKenzie

Structural controls on Tertiary orogenic gold mineralization during initiation of a mountain belt, New Zealand

Received: 11 April 2006 / Accepted: 9 August 2006 / Published online: 23 September 2006

Abstract Two types of structurally controlled hydrothermal mineralization have occurred during folding of fissile schist in southern New Zealand: fold-related mineralization and normal fault-related mineralization. Both types have the same mineralogy and textures, and are dominated by quartz–ankerite veins and silicified breccias with ankeritic alteration. Most mineralized zones are thin (centimetre scale), although host schist is commonly impregnated with ankerite up to 20 m away. Thick (up to 5 m wide) mineralized zones are generally gold-bearing and contain pyrite and arsenopyrite with stibnite pods locally. Some of these auriferous zones have been extensively mined historically despite rugged topography and difficult access. Mineralization occurred during regional tectonic compression in the initial stages of development of the Southern Alps mountain belt at the Pacific–Australian plate boundary in the Miocene. Most of the gold-bearing deposits occur in east to south-east, striking normal faults that cut across mesoscopic folds in a belt that coincides with the southern termination of a regional-scale north trending antiform. Mineralized zones have similar structural control and relative timing to a nearby swarm of Miocene lamprophyre dykes and carbonatites. Limited stable isotopic data (C and O) and trace element geochemistry suggest that there was probably no genetic link between the igneous activity and gold mineralization. However, these two types of fluid flow have been controlled by the same tectonically created crustal plumbing system. This Miocene hydrothermal activity and gold deposition demonstrates that orogenic (mesothermal) mineralization can occur during the inception of an orogenic belt, not just in the latter stages as is commonly believed. These Miocene structures have been preserved in the orogen because the locus of uplift has moved northwards, so the early-formed gold deposits have not yet been structurally overprinted or eroded.

Keywords Gold · Lamprophyre · Orogenic · Mesothermal · Hydrothermal · Tectonic · Fold

Editorial handling: N. White

D. Craw (✉) · M. Begbie · D. MacKenzie
Geology Department, University of Otago,
P.O. Box 56 Dunedin, New Zealand
e-mail: dave.craw@stonebow.otago.ac.nz

Introduction

Orogenic (mesothermal) gold deposits have formed in a range of structural settings in collisional mountain belts throughout geological time (Goldfarb et al. 2001; Groves et al. 2003). The economically most productive of these deposits formed in ancient mountain belts that are now exposed after long-term deep erosion to the middle crust (Bierlein and Crowe 2000; Goldfarb et al. 2001; Groves et al. 2003). These ancient deposits have been variably dismembered and structurally overprinted by younger events so that details of the structural setting in which the deposits formed have been obscured. On the other hand, many young and/or active mountain belts have evidence for orogenic-style gold deposit formation, and the structural setting for such deposits is readily discernible (Nesbitt et al. 1986; Goldfarb et al. 2001; Craw et al. 2002). However, almost all of these young deposits are small and of negligible economic interest, and merely indicate the probable occurrence of larger deposits not yet exposed in the orogens (Nesbitt et al. 1986; Craw et al. 2002).

The South Island of New Zealand is a unique orogenic belt in that it hosts both ancient (Mesozoic) and modern orogenic gold deposits in close proximity in the same host rock suite (Fig. 1; Craw and Norris 1991; Craw and Campbell 2004). The details of the structural and tectonic setting of the Mesozoic deposits, including the world-class Macraes deposit (c. 150 t Au) have long since been eroded and overprinted so only general inferences on the regional structural controls on mineralization can be made (Teagle et al. 1990; Craw and Norris 1991). The gold mineralizing systems in the active orogen can be accurately defined from structural and tectonic perspectives (Fig. 1), but the

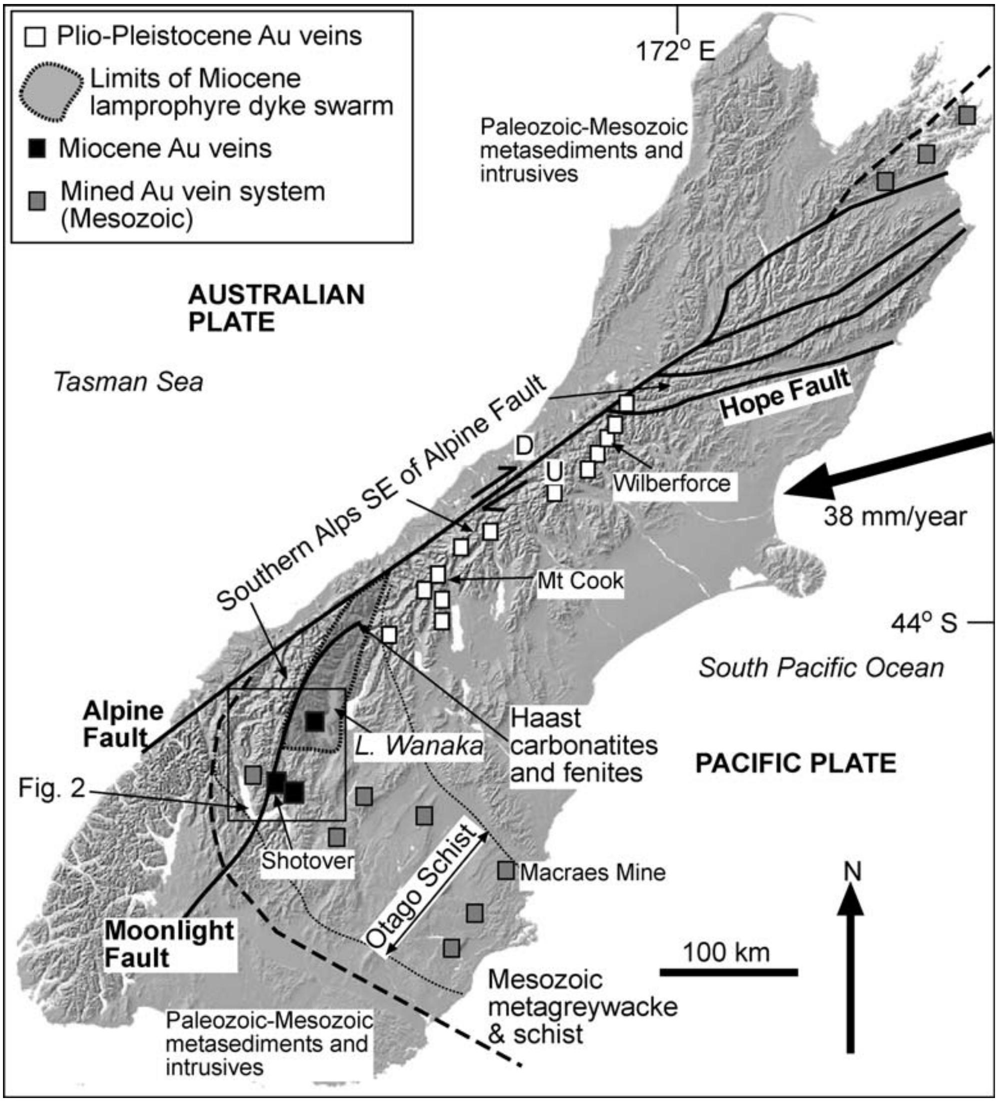

Fig. 1 Digital elevation model (from http://Geographx.co.nz) of the South Island of New Zealand showing the Southern Alps orogen in its current tectonic setting (see text). Locations of principal Mesozoic, Miocene and Plio-Pleistocene gold-bearing deposits are indicated

resulting deposits are trivial in scale. However, a set of gold deposits that do have some economic significance is exposed between the ancient and modern deposits, and these deposits formed in the early (Miocene) stages of development of the modern orogen (Fig. 1). These intermediate gold deposits, the topic of the present study, have been exposed by erosion of the oldest part of the active orogen. Thus, these Miocene deposits are ideal for study of regional structural controls on gold mineralization because they have almost all evidence of their structural setting preserved but are sufficiently deeply eroded to expose an economically important structural level. Furthermore, these deposits show that gold mineralization occurred during the inception of the modern orogen, not just in the latter stages as is commonly believed (Goldfarb et al. 2005).

Lamprophyre dykes are commonly found closely associated, both temporally and spatially, with orogenic gold deposits (Taylor et al. 1994; Kerrich and Wyman 1994; Ashley et al. 1994). This close association may be indicative of a genetic link between gold and lamprophyres (Rock et al. 1989). However, most workers believe that the gold–lamprophyre association is merely structural, with both using the same conduits for migration through the crust (Taylor et al. 1994; Kerrich and Wyman 1994; Ashley et al. 1994). In this study, gold-bearing veins and lamprophyre dykes are in close proximity, and their regional structural relations can be readily assessed in this young orogen. Study of the controls on mineralization in these Miocene veins is further simplified by the absence of igneous bodies (other than lamprophyres) that serve to complicate studies of orogenic gold in most other belts, both ancient and modern (Groves et al. 2003).

In this study, we describe the structural controls on hydrothermal gold mineralization in highly fissile and folded schists. We also describe this mineralization in the context of regional structural evolution of the hosting portion of the young orogen. We show that mineralization occurred during the earliest stages of development of the orogen. The mineralization occurred at the same time as lamprophyre dykes were being intruded nearby, but we show that there is no direct genetic link between gold and lamprophyres.

General geology

Tectonic setting

The South Island of New Zealand is made up of numerous accreted terranes, including the Mesozoic metagreywacke terranes of the eastern (E) part of the island, which are the focus of this study (Fig. 1). The metagreywackes contain minor interlayered argillaceous metasedimentary rocks and relatively massive metabasic horizons. The Mesozoic metagreywacke rocks range from zeolite to greenschist facies, with the greenschist facies rocks occurring principally in a schist belt (Otago Schist) and along the axial mountains (Fig. 1). Some metagreywacke, including greenschist facies schist, has been offset nearly 500 km by dextral motion on the Alpine Fault (Fig. 1). The South Island lies astride the active tectonic boundary between the Pacific and Australian plates, with a relative plate vector oriented south-west (SW) at 38 mm/year (Fig. 1; DeMets et al. 1994). The transpressional Alpine Fault is the plate boundary on land, and uplift on the south-east (SE) side of this fault has formed the Southern Alps, the main axial mountains along the island (Fig. 1). Maximum uplift rates are up to 8 mm/year in the central Southern Alps (SW of Mt. Cook, Fig. 1; Simpson et al. 1994), and uplift rates decrease to the north-east (NE) and SW (Wellman 1979).

The current plate boundary began to develop in the early Tertiary during readjustment of plate geometry in the SW Pacific (Carter and Norris 1976), and the Alpine Fault was initiated as a through-going structure in the Miocene (Fig. 3; Cooper et al. 1987). The mountains began to develop to the west of Lake Wanaka (Figs. 1, 2) at that time, grew northwards to form the present 500-km-long axial chain in the late Miocene and Pliocene, and continued to rise through the Pleistocene to the present (Fig. 3; Norris et al. 1990; Craw 1995). A prominent subsidiary fault, the Moonlight Fault (Figs. 1, 2 and 3), was active as an extensional structure in the Oligocene, controlling localized deposition of marine and non-marine sediments (Fig. 3; Turnbull et al. 1975). The Moonlight Fault became a reverse structure in the Miocene during inception of the Alpine Fault (Craw 1985; Cooper et al. 1987). The Moonlight Fault is still active, although only minor (metre-scale) Quaternary motion has been documented (Turnbull 2000), and uplift rates are c. 1–2 mm/year in the area of this study to the SW of Lake Wanaka (Fig. 2; Wellman 1979).

Dykes and gold-bearing hydrothermal zones

A prominent set of alkaline lamprophyre dykes was intruded into extensional fractures during the Miocene inception of the Alpine Fault (Figs. 1, 3; Cooper et al. 1987). These dykes have predominantly E or SE strikes, with some striking NE, and generally fill fractures at a high angle to coeval north (N) to NE trending folds (Craw 1985; Cooper et al. 1987). Dykes occur sporadically through the area to the west of Lake Wanaka and northwards towards the Alpine Fault in a swarm with mappable boundaries (Figs. 1, 2 and 3). The dykes occur only to the E of the Moonlight Fault, but some occur within and immediately west of a related fault at the northern end of the Moonlight Fault (Craw 1985). Carbonatite dykes occur associated with the lamprophyre swarm in the Haast River area (Fig. 1; Cooper 1986). The host schist has been locally fenitised along the margins of carbonatites (Cooper 1986; Paterson 1992). Farther south, ankeritic alteration commonly occurs in host schist along lamprophyre dyke margins and in nearby fractures, particularly fractures with E and SE strike (Craw 1985, 2006). This alteration is locally accompanied by thin (<20 cm) quartz veins and/or breccias with minor silicification.

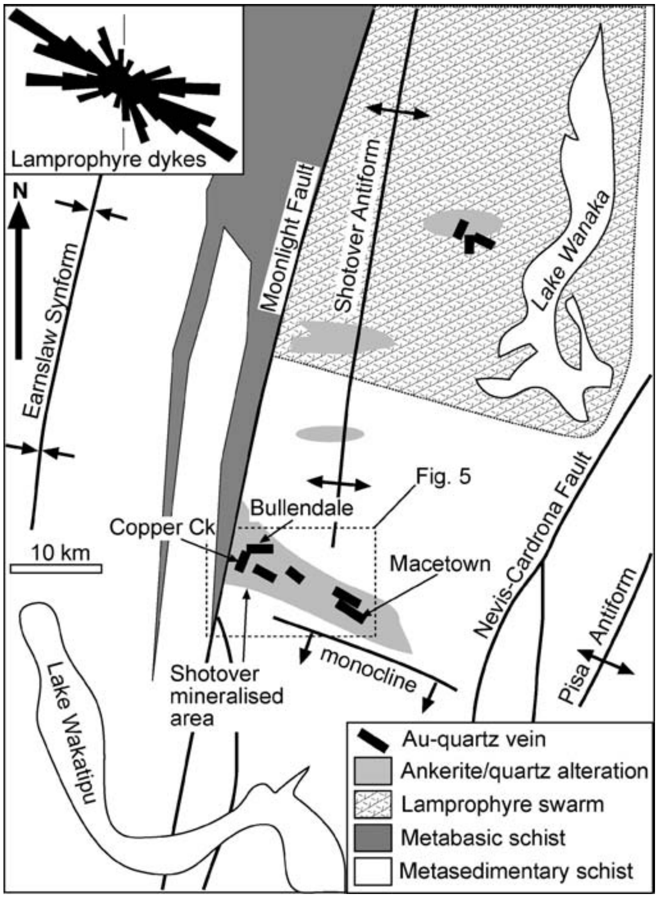

Fig. 2 Structural map of the southern end of the Southern Alps (see *box*, Fig. 1) showing the principal folds and faults relevant to the present study. Structurally controlled lamprophyre dykes and ankerite/quartz alteration occur scattered sparsely through ornamented areas as indicated. *Inset* shows a *rose diagram* of strikes of lamprophyre dykes in the areas west of Lake Wanaka (after Cooper et al. 1987)

Gold-bearing hydrothermal deposits occur principally in greenschist facies rocks, and locally in lower grade rocks, through the Mesozoic metagreywackes (Fig. 1; Craw et al. 2002). The economically most important of these deposits, including the Macraes deposit (>100 t Au), formed in the latter stages of Mesozoic metamorphism and associated uplift (Fig. 1; Craw 2002). Most of these zones formed in the middle crust and have been exposed by deep erosion

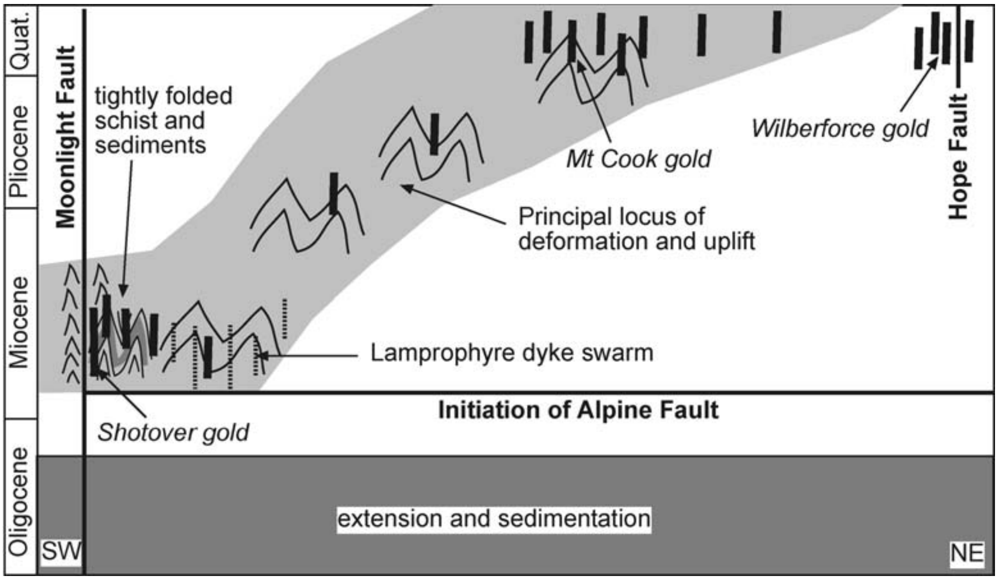

Fig. 3 Sketch space–time plot (not to scale) for the Southern Alps from the Moonlight Fault in the Shotover area (*left*) to the Hope Fault (*right*) based on observations from Craw (1995), Teagle et al. (1998), Craw and Campbell (2004), and Craw (2006). The principal locus of uplift and deformation (*light grey*) has moved northeast with time since initiation of the orogen with the inception of the Alpine Fault. Moonlight Generation folds, and similar but later folds elsewhere, are indicated with *wavy lines*. Relative timing of emplacement of gold-bearing veins (*heavy black lines*) and lamprophyre dykes (*dashed lines*) is indicated

that accompanied unroofing of the schist belt in the Cretaceous (Craw and Norris 1991; Gray and Foster 2004). In contrast, a set of non-economic vein gold occurrences occurs near the crest of the Southern Alps (Figs. 1, 3; Craw and Campbell 2004). These veins formed at relatively shallow levels (mostly upper 2 km) associated with the tectonically driven fluid flow system accompanying the Plio–Pleistocene rise of the Southern Alps (Teagle et al. 1998; Craw and Campbell 2004). A related set of veins, centred on the Wilberforce area, was emplaced in a regional deformation zone at the intersection of the Alpine Fault with the strike-slip Hope Fault (Figs. 1, 3; Craw and Campbell 2004).

The hydrothermal zones that are the topic of the present study occur in the region in which the Southern Alps uplift began in the Miocene (Fig. 3; Craw 1995), and several kilometres of subsequent erosion has exposed the zones in an area of steep relief. Auriferous deposits in the Shotover and Macetown areas (Fig. 4) were extensively mined from the 1870s to the early 1900s via underground tunnels following the well-defined mineralized zones (Williams 1974). The economically most important deposit at Bullendale (Fig. 3) produced about 1 t of gold with grades as high as 45 g/t (Williams 1974). Some of the smaller deposits in the Shotover–Macetown area have not been mined or have had negligible production. Several unsuccessful attempts have been made over the past 30 years to define viable ore bodies in the Shotover and Macetown areas (Begbie and Craw 2006). Auriferous veins immediately west of Lake Wanaka (Figs. 1, 2 and 3) are small and have not been mined.

Methods

This study takes advantage of up to 1,500 m of steep relief in actively eroding mountains (Figs. 4, 5) to provide natural outcrops of hydrothermal alteration zones, including auriferous deposits. These natural outcrops provide a detailed view of the anatomy of hydrothermal zones in three dimensions in their original structural context. Much of this study is based on direct observations of the structures in these outcrops, particularly near the Moonlight Fault where structural relations are most clearly exposed. Because of the remote and rugged nature of the terrain, some auriferous zones have not been mined or were mined historically from surface outcrops and stream boulders only. The observations of rugged natural outcrops are augmented by structural observations from accessible historic mine tunnels at lower altitudes and the natural outcrops that surround these mine sites.

Samples of mineralized rock were collected from natural outcrops (particularly well exposed in Copper Creek), historic mine workings and drill core from the Bullendale mining area (Figs. 2, 4). Transmitted and incident light microscopic observations of mineralogy and textures were made on fresh material from outcrops and drill core. Mineral identifications were confirmed with an electron microprobe. X-ray fluorescence analyses of mineralized rocks were obtained from SpectraChem Analytical, Wellington, New Zealand. Detailed geochemical interpretation of these analyses is beyond the scope of this study, but the analyses are used for comparison with fenite alteration associated with carbonatites described by Cooper (1986) and Paterson (1992).

Structural setting of the Miocene gold deposits

Uplift associated with the initiation of the Southern Alps has exposed a deeper portion of the schist belt, the Aspiring Terrane, which hosts the gold deposits of this study (Norris and Craw 1987). The Aspiring rocks are dominated by highly fissile mica-rich metasedimentary schists, with subordinate (up to 20%) interleaved metabasic schists (Norris and Craw 1987).

The Otago Schist has a pervasive foliation that is generally flat-lying or shallow-dipping. The schist foliation

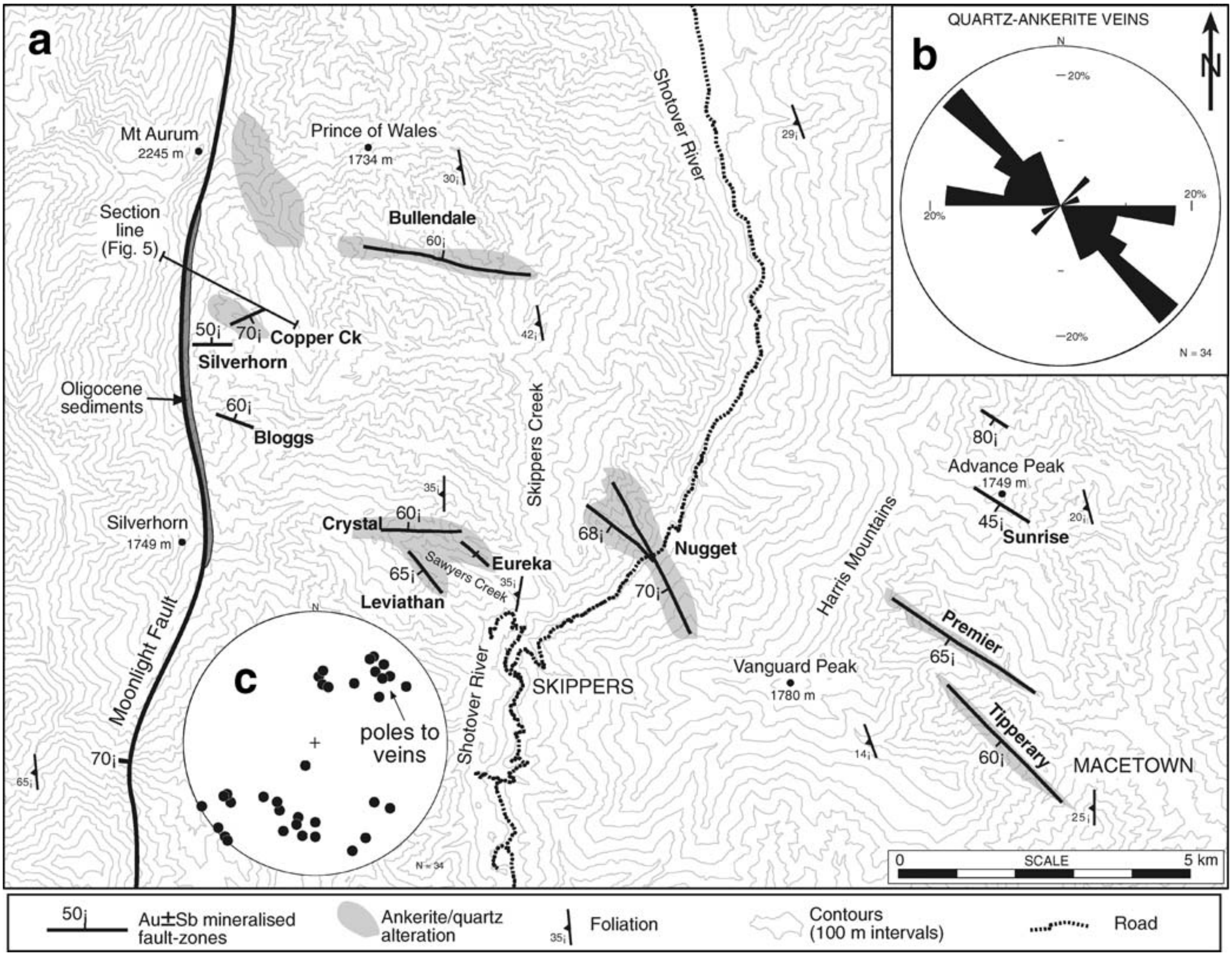

Fig. 4 a Geological and topographic map of the Shotover–Macetown area (see Fig. 2). Principal gold- and/or stibnite-bearing mineralized zones are shown with *heavy lines*. Names attached to most of these are from historical mining records. Ankerite/quartz alteration occurs scattered sparsely through the grey areas around mineralized zones and is not pervasive. **b** *Rose diagram* of strikes of quartz–ankerite veins and breccia zones for comparison with *inset* in Fig. 2. **c** Stereonet (lower hemisphere) showing poles to quartz–ankerite veins

has been folded into broad N to NE trending synforms and antiforms (10–20 km wavelength) near to, and associated with, the Moonlight Fault (e.g. Earnslaw Synform, Shotover Antiform; Fig. 2; Craw 1985; Cooper et al. 1987). Similar regional folds but with NE trend such as the Pisa Antiform (Fig. 1) are Quaternary structures (Jackson et al. 1996). Mesoscopic open to tight upright folds of foliation occur throughout fissile metasedimentary schist adjacent to the Moonlight Fault and in zones within the broad regional folds (Figs. 2, 5). These mesoscopic folds have N to NE trends, parallel to the adjacent Moonlight Fault and to broad regional folds related to that fault, and were described as a distinct "Moonlight Generation" by Craw (1985). Zones of these mesoscopic folds were formed in close proximity to the Moonlight Fault during its Tertiary reverse-movement phase. This generation of mesoscopic structures was initiated with their macroscopic counterparts during the inception of the Moonlight Fault in the Miocene (Craw 1985; Cooper et al. 1987). The immediate hanging wall of the Moonlight Fault consists of a thick (50–500 m) slab of metabasic schist for much of its length west of Lake

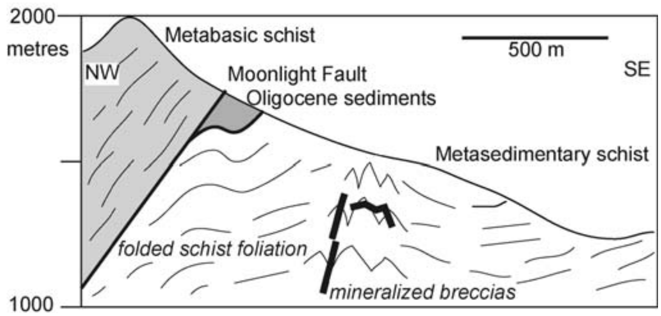

Fig. 5 Sketch cross section through the Copper Creek area (Fig. 4) partly after Turnbull et al. (1975). Structural relations between Oligocene sediments, the underlying metasedimentary schist and gold-bearing deposits are indicated, as well as the Moonlight Fault and a thick slab of metabasic schist in the hanging wall

Wanaka (Fig. 2). This metabasic schist is less fissile than the metasedimentary schists in the footwall, and mesoscopic Moonlight Generation structures are less prominent (Fig. 5). Gold-bearing veins described in the present study occur intimately associated with Moonlight Generation structures in the footwall of the Moonlight Fault.

Oligocene sediments deposited along the ancestral Moonlight Fault zone in an extensional environment have been deformed during Miocene reversal of the fault (Turnbull et al. 1975). Remnants of these sediments are now preserved as thin slivers (typically <100 m thick) on the footwall of the Moonlight Fault (Figs. 3, 4 and 5). The basal sedimentary contact on the underlying schist is preserved locally and lies subparallel to the schist foliation (Turnbull et al. 1975). The sediments, the basal contact and the underlying schist foliation have been folded by Moonlight Generation folds (Fig. 5) with localized shearing of the basal sedimentary contact. The Moonlight Generation folds of schist foliation form a uniform set of structures that are traceable from immediately beneath the folded sediments both down-section and laterally to the E for at least 5 km. This close relation between deformed Oligocene sediments and Moonlight Generation structures is an important strand of evidence used to date the Moonlight Generation structures as mid- to late-Tertiary (Craw 1985). The age of these structures is confirmed further N by their close association with the intrusion of the lamprophyre dyke swarm that has been dated radiometrically by several methods as Miocene (20–25 Ma; Cooper et al. 1987).

Deposit geology and structure

Mineralogy

There are two distinct but related types of hydrothermal zones: zones that formed in close association with Moonlight Generation folds and zones that formed in faults at a high angle to Moonlight Generation structures. Both types of zones have the same mineralogy, as described below, and both had similar textures during mineralization. Some of the fold-related zones have been folded and disrupted by their host folds. Likewise, the fault-related zones have been deformed by continued movement of their host faults. This post-depositional deformation has modified some textures, but the mineralogy has remained unchanged despite minor remobilization of quartz and ankerite.

The hydrothermal zones consist of silicified schist breccias and subordinate quartz veins, with some open cavities and prismatic quartz crystals. Most of the breccias are hydrothermal in origin, with abundant quartz cementing scattered clasts rather than cataclastic breccias. Thin (up to 5 cm) seams of grey to black silicified cataclasite occur along fault zones. Ankeritic carbonate is abundant in all hydrothermal zones, weathering to a distinctive orange-brown colour that is visible over hundreds of square metres of some outcrops. Some of the ankeritic carbonate is vein-filling material, and some is a result of hydrothermal alteration of host schist chlorite to kaolinite. The ankeritic carbonate has penetrated up to 100 m beyond principal mineralized zones, and minor silicification also accompanies this host rock alteration. The ankeritic alteration halo is strongly structurally controlled by schist foliation, joints, and fractures, and the areas indicated in Figs. 2 and 4 are not pervasively altered. Hydrothermal albite occurs in some veins with quartz and ankeritic carbonate. The hydrothermal alteration has resulted in three- to sixfold enrichment in Sr (up to 600 ppm) principally associated with ankerite (Craw et al. 1991).

Pyrite and arsenopyrite are abundant in the most intensely altered and variably silicified breccia and vein zones, locally constituting up to 20% of the mineralized rock. Gold is closely associated with these sulphide minerals as free grains up to 3 mm and as micron scale blebs enclosed in sulphide grains. Lenticular masses of vein quartz (metre scale) occur sporadically along the mineralized zones. Pods up to 1 m long and 30 cm thick of massive stibnite occur within some mineralized zones. The stibnite occurs in close proximity (centimetre scale) to arsenopyrite-bearing rock, but arsenopyrite and stibnite do not coexist. All gold-bearing deposits occur near the cores of zones with abundant ankerite–quartz alteration, but many ankerite–quartz alteration zones do not contain auriferous sulphides (Fig. 2).

Fluid inclusions

Fluid inclusion geothermobarometry was not part of the present study because this has been published previously (Craw 1989), and the following account is a summary of that work relevant to this study. Quartz crystals that are texturally younger than auriferous sulphide-rich zones have abundant two-phase aqueous fluid inclusions that typically homogenize to liquid at 145–175°C (Craw 1989). Ice-melting temperatures are between −1 and −1.6°C, consistent with low-salinity fluids. In addition, there are relatively rare three-phase CO_2-rich inclusions, including some inclusions with only a thin annulus of H_2O liquid phase around a CO_2-rich interior (Craw 1989). These CO_2-bearing inclusions coexist with the aqueous inclusions, suggesting localized fluid immiscibility during mineralization (Craw 1989). Fluid immiscibility phase equilibria, associated with geometrical reconstruction of the pre-erosion surface, suggest that mineralization occurred in the upper 2–4 km of the schist during the Miocene (Craw 1989).

Structure of fold-related hydrothermal zones

Fold-related hydrothermal zones occur irregularly through the Shotover–Macetown area, particularly in belts of relatively intense Moonlight Generation folding near the Moonlight Fault. These zones are controlled by the geometry of the Moonlight Generation folds and have N to NE strike, subparallel to the trends of the folds. Veins and alteration zones range in thickness from centimetre scale to 10-metre scale. Quartz–ankerite veins (up to 30 cm thick) filling fractures parallel to fold axial surfaces (Fig. 6a,c) are the most common. These thin veins are discontinuous on the centimetre-to-metre scale (Figs. 6b,c, 7a). Some of these thin veins deviate into parallelism with the folded foliation (Fig. 6a). Similar quartz–ankerite veins fill fractures perpendicular to the fold axes, and some of these are laminated on the millimetre scale. These perpendicular veins have been bent, and laminations disrupted, by folding-related deformation.

A thick (metre scale) auriferous silicified breccia zone in Copper Creek was partially emplaced within fold axial surface fractures and partly emplaced parallel to the schist foliation (Figs. 6b,c, 7a). Associated fold axial surface fractures contain thin quartz–ankerite veins (Figs. 6c, 7a). Foliation in schist clasts within the silicified breccia is variably folded in a similar manner to the host schist (Moonlight Generation), and these clasts of folded schist became rotated during brecciation (Figs. 6c, 8a). Arsenopyrite and pyrite alteration occurs in and near breccia clasts (Fig. 8a,b), and stibnite pods occur within the breccia matrix. Some breccia fragments have been repeatedly fractured and recemented with quartz. The whole silicified breccia has been folded by the same Moonlight Generation structures that controlled its initial emplacement (Fig. 6b,c). Poles to the marginal surface of the silicified breccia define a great circle with a fold axis plunging moderately NE (Fig. 6d). Flexural slip folding of the breccia zone has resulted in millimetre-scale striae on the margins, plunging gently ESE (Fig. 6d). Folding of the silicified breccia has resulted in fractures in the fold hinge zone. Some of these fractures have been filled with quartz and ankerite veinlets, forming a network of cross-cutting stringers (Fig. 6c).

Large (1- to 10-m scale) steeply dipping auriferous silicified breccias occur immediately upstream of the folded breccia in Copper Creek (Fig. 4). These silicified breccia zones have similar mineralogy and textures to the nearby folded silicified breccia, including abundant arsenopyrite and stibnite (Figs. 7b, 8b), and are traceable discontinuously for up to 30 m up-section at the western edge of a zone of tight Moonlight Generation folds (Fig. 5). Moonlight Generation folds trend NE in this folded zone, and the schist foliation dips mainly NW (Figs. 5, 9a,b). The steeply dipping silicified breccias fill fault zones that strike NE to ENE, locally subparallel to Moonlight Generation

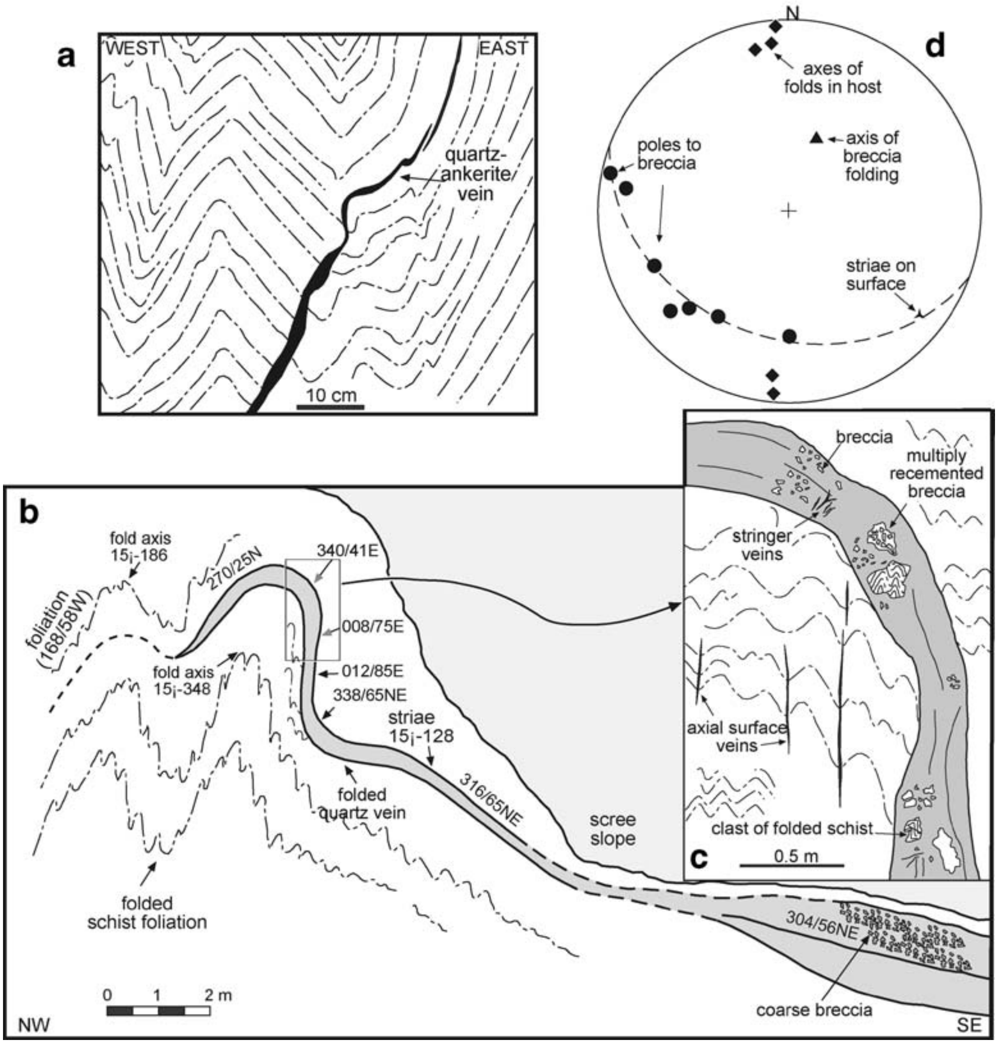

Fig. 6 Fold-related mineralized veins and breccias. **a** Sketch (from photograph) of quartz–ankerite vein (*black*) in fold axial surface of Moonlight Generation folds. **b** Sketch (from photograph montage) of a gold-bearing silicified breccia and vein zone (*grey*) in Copper Creek (Figs. 2, 3). Moonlight Generation folds of foliation (*light lines*) have controlled emplacement of, and subsequently folded, the breccia zone. **c** Enlarged portion of **b** (see *box*) showing details of the structural relations between breccia zone and folds (see text). **d** Stereonet (lower hemisphere) of principal structural elements of the breccia zone in **b** (see text)

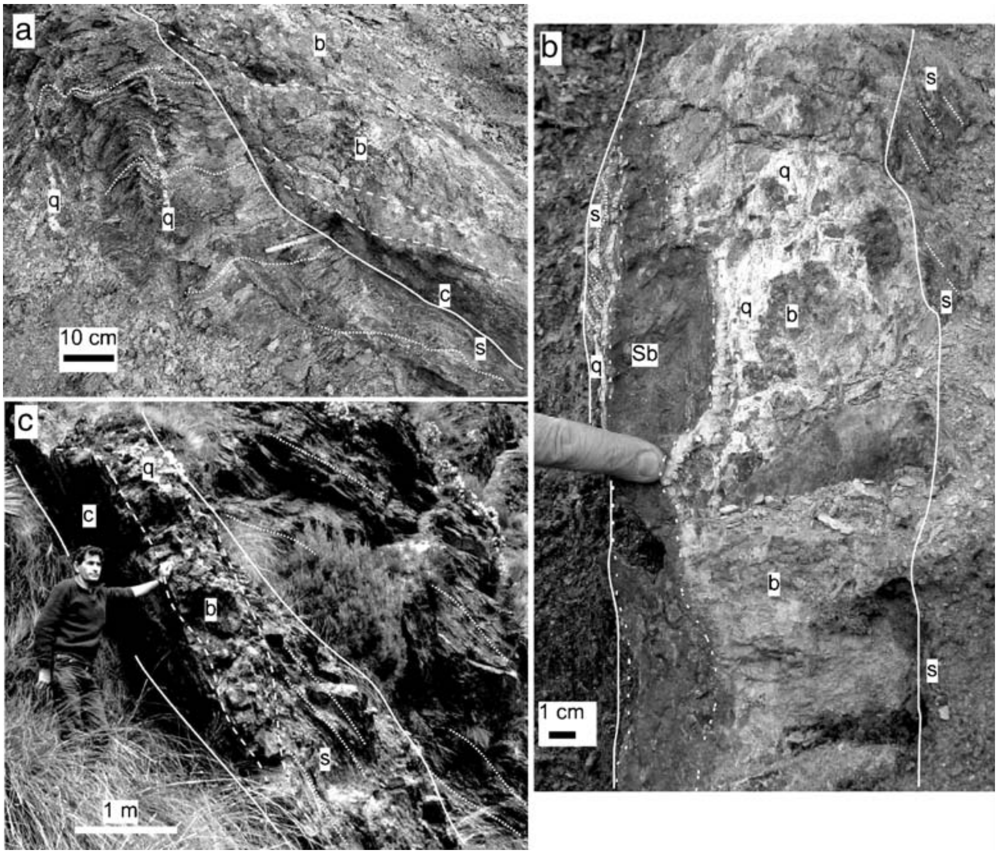

Fig. 7 Outcrop photographs of mineralized zones in the Shotover area showing schist foliation (*dotted white lines*), mineralized zone margins (*solid white lines*) that locally have cataclasite (*c*) and internal shears (*dashed white lines*). Mineralized zones contain sheared schist (*s*) and breccias (*b*), with localized stibnite (*Sb*). Quartz veins and cement (*q*) occur within host schist and in breccias. **a** Silicified breccias (*right*) in the Copper Creek folded mineralized zone truncate Moonlight Generation fold in the host schist (*left*). Thin hydrothermal quartz veins (*q*) fill fold axial surfaces in host schist. **b** Mineralized breccia in a normal fault, Copper Creek, with massive Sb (*white dotted margin*). Breccia clasts (*grey*) are cemented with q (*white*). **c** Mineralized normal fault at Bloggs locality (Fig. 5). The footwall surface is exposed as a thin (<5 cm) silicified zone c beneath breccias and sheared schist

fold axial surfaces, but generally are slightly oblique to the folds (Figs. 7b, 9a,b). Thin cataclastic breccias along faults are silicified and impregnated with sulphides (Fig. 9c). Strongly deformed and disrupted schist is broken into metre-scale blocks with varying foliation orientations, and localized breccia zones with centimetre-scale clasts are cemented with quartz (Figs. 7b, 9a,d). Schist blocks and breccia clasts are generally tightly folded with Moonlight Generation structures that commonly retain their original fold axis trends. The schist blocks and breccias are variably silicified and impregnated with ankerite and sulphides (Fig. 8a,b). Quartz veins are rare and thin (centimetre scale), and are dominated by silicified breccia clasts (Fig. 9a,e). Polished surfaces on fault planes have striae that plunge steeply down-dip (Fig. 9b). Bending of schist foliation adjacent to fault planes suggests a normal sense of motion on the faults (Fig. 9a).

Structure of fault-related hydrothermal zones

Fault-related hydrothermal zones occur along well-defined steeply dipping faults that strike predominantly E and SE, with rare faults striking NE (Fig. 4a–c). All of the historically mined gold deposits apart from Copper Creek (Figs. 4, 6) occur in these fault zones. In addition, some unmined auriferous zones and a large non-auriferous zone of alteration near Mt. Aurum (Fig. 4) are hosted by these faults. The faults cut sharply across the Moonlight Generation folds, and these folds have been locally deformed and reoriented by fault-related shearing (Fig. 10). Fault zones are similar to those described in the previous section (Fig. 9) but are more discordant to the Moonlight Generation structures and the schist foliation that strikes subparallel to the general N to NE fold axial trend (Fig. 7c). Fault zones are sharply bounded on both their hanging wall and footwall by relatively undisturbed wall-rock schist (Figs. 7c, 10). Slip occurs throughout the fault zone, as indicated by many internal discrete and often discontinuous faults (Figs. 7c, 10). Fault rocks consist of gouge up to several centimetres thick, crushed and folded schist, stockwork veins, cataclasite bands and brecciated wallrock.

Hydrothermal alteration, breccias and veins are structurally controlled by the faults and have the same strike and dip (Fig. 10). Veins and silicified breccias form resistant masses within the fault zones that subsequent faulting has cut and/or bent around. Early-formed veins and breccias have later polished fault surfaces imposed on them, with thin (centimetre-scale) cataclasite and gouge seams. Some of the cataclasite and gouge seams have in turn been silicified and mineralized with sulphides. Slickensides on fault surfaces generally indicate a dip-slip sense of movement (Fig. 11a,b). The foliation in intact rock is progressively rotated towards the fault margins over several metres (Figs. 7c, 9a, 10). This relation between mineralized fault zones and host schist foliation is consistent across the whole study area and indicates a normal sense of separation. This inferred sense of normal separation is consistent with development of steep open

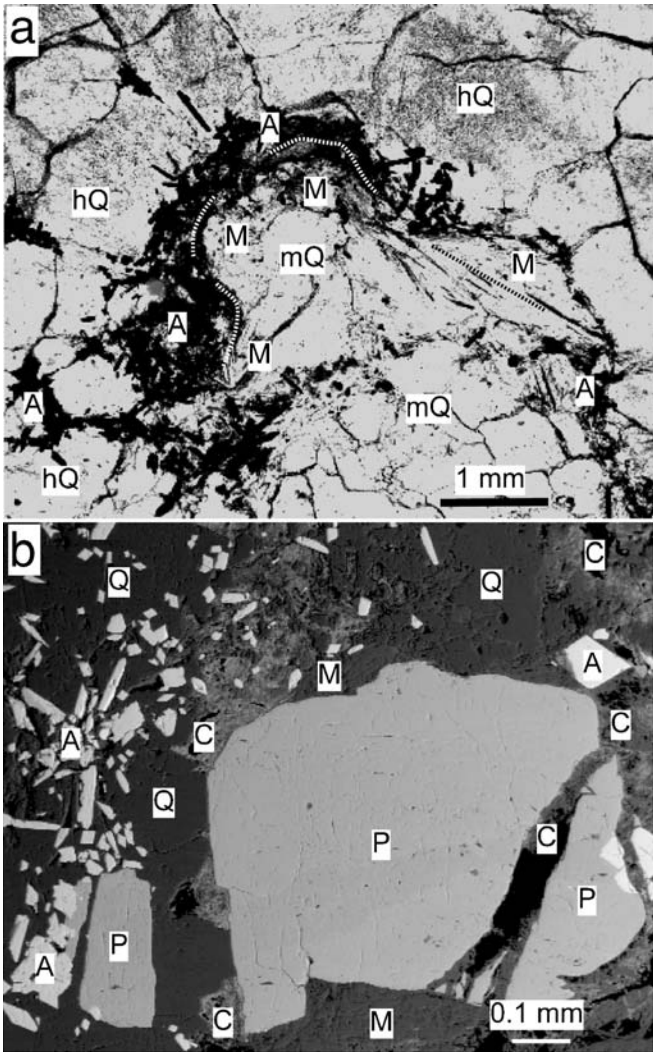

Fig. 8 Microscopic images of mineralized rocks from Copper Creek mineralized zones. **a** Transmitted light view of a schist breccia clast containing anhedral metamorphic quartz (*mQ*) and M, and cemented by euhedral hydrothermal quartz (*hQ*). Quartz grain boundaries have been accentuated after carbon-coating for microprobe examination but also host some A (*black*) The M-rich foliation in the clast has been folded (Moonlight Generation), as indicated with *dotted lines* (*white* on *left* and *top*; *black* on *right*). Hydrothermal arsenopyrite impregnates the clast around its margin, particularly the M-rich portions. **b** Backscatter electron image of silicified and mineralized schist adjacent to a quartz vein. Sulphides are dominated by coarse pyrite (*P*) and fine arsenopyrite (*A*) dispersed through hydrothermal and metamorphic quartz (*Q*) with minor metamorphic muscovite (*M*). Hydrothermal ankeritic carbonate (*C*) occurs as pools and veins

fractures that have been partially filled with breccia and introduced quartz cement.

Some faults have kink folds in the deformed zones on their immediate margins (up to 1 m wide). These kink folds have axes subparallel to the strike of the adjacent fault, and the kinks deform Moonlight Generation folds. Quartz–ankerite veins, breccias and cataclasite seams occur along some kink fold axial surfaces (Fig. 11a). Striae on the fold axial surface vein in Fig. 11a plunge shallowly E (Fig. 11b) and are a result of flexural slip deformation during kink folding. This is in contrast with the more northerly plunge of striae on the associated mineralized fault (Fig. 11a,b).

Discussion

Mineralization during regional compression

The structures described above for the fold-related hydrothermal zones demonstrate that mineralization occurred during regional compressional deformation. The folds developed in the footwall of a major regional reverse fault and are genetically linked to that fault because they also deform the faulted slivers of Oligocene sediments (Fig. 5). Hence, it is clear that hydrothermal fluid flow and associated gold mineralization were initiated during the reverse phase of movement on the Moonlight Fault. Despite the overall compressive strain regime, there is abundant evidence for extensional deformation, including vein emplacement (Fig. 6a), hydrothermal brecciation (Figs. 6b,c, 9, 10) and normal fault movement (Figs. 9a,b, 10, 11). These extensional sites developed locally within the folding rock mass, permitting emplacement of mineralized material, including auriferous sulphides.

Most of the auriferous zones are hosted in normal faults (Fig. 4), but the Copper Creek folded silicified breccia may have formed as a saddle reef in an evolving fold hinge (Fig. 6b). This style of mineralization resembles some aspects of the well-studied Bendigo–Ballarat goldfield, Australia, where mineralization accompanied flexural-slip folding of well-bedded turbidites during horizontal compression (Cox et al. 1991; Sibson and Scott 1998). Veins and breccias in these Australian examples also extend along bedding planes locally in a similar manner to the foliation-parallel silicified breccia in Copper Creek (Fig. 6b). However, the fold-related cross-cutting mineralized extensional faults in Copper Creek (Fig. 9) appear to have normal sense of motion (above) in contrast with mineralized reverse faults that accompanied saddle reef formation in the Australian example. It is possible that these mineralized faults in Copper Creek may have been initiated as reverse structures during tight Moonlight Generation folding and were reactivated as normal faults at the same time as the other mineralized normal faults formed nearby (Fig. 4).

Formation of extensional sites during regional compression in the Shotover–Macetown area was apparently controlled by folding in the highly fissile foliated host schist, as in the well-bedded turbidites of Bendigo and Ballarat (above; Cox et al. 1991; Sibson and Scott 1998). These extensional sites do not form in more massive rocks such as those in Archean terranes, where compression-related extensional sites are strongly related to reverse faults rather than folds (Sibson et al. 1988; Witt and Vanderhor 1998).

The Moonlight Fault has remained a reverse structure since the Miocene and is still active as such. Nevertheless, fold-related hydrothermal zones have been cut by mineralized normal faults at a high angle to the N to NE

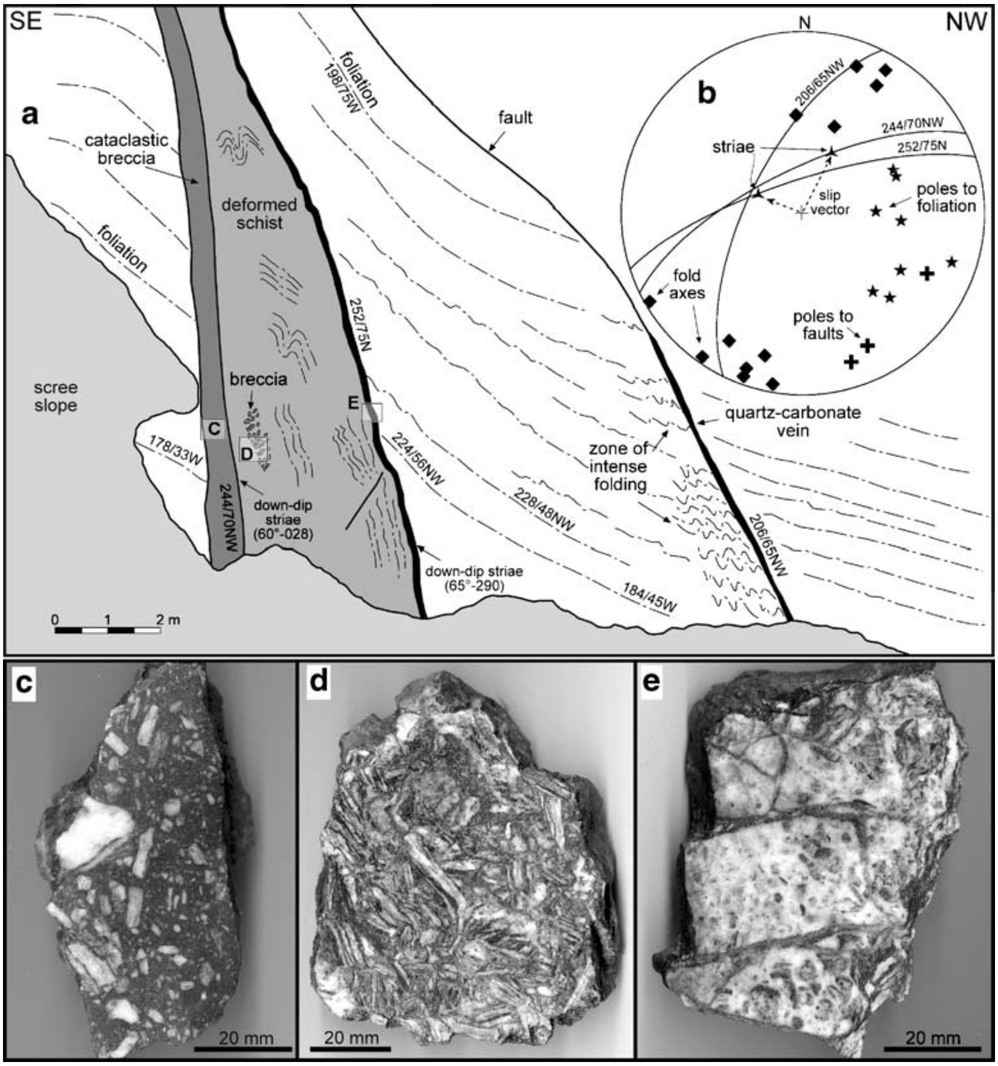

Fig. 9 Structural features of a steeply dipping gold-bearing breccia zone associated with the folded breccias in Copper Creek (Fig. 5). **a** Sketch (from photo montage) of outcrop showing the relations between cataclastic breccia (*dark grey*), deformed schist and associated breccias (*light grey*) and veins (*black*), faults, folds and foliation. **b** Stereonet (lower hemisphere) of the principal structural elements in the outcrop (see text). **c**–**e** Photographs of breccia samples taken from the indicated sites in **a**

structural grain of the region (Figs. 2, 4). However, apart from small occurrences west of Lake Wanaka, all the gold-bearing deposits, including the historical producers, are located in a SE trending belt between the Moonlight Fault and Macetown (Fig. 2). This belt coincides with the southern termination of the Shotover Antiform, a Moonlight Generation regional structure (Fig. 2). South of this fold termination, the schist foliation dips southwards in a regional monocline that may have been present before development of the Moonlight Generation. Hence, it is possible that extensional faulting and fracturing occurred in this structural transition zone between Shotover Antiform and the regional monocline.

It is notable that all the hydrothermal zones and associated gold deposits occur only in the footwall of the Moonlight Fault (Figs. 2, 5). Extensive quartz–carbonate veining and alteration occurs almost to the fault in several places, especially near Mt. Aurum (Fig. 4a), yet none occurs in the hanging wall. One explanation for this may be that the massive metabasite slab in the hanging wall, combined with the cataclasites of the fault zone itself, have formed an impermeable barrier to passage of hydrothermal fluids. Certainly, the massive metabasite is only weakly affected by Moonlight Generation folding, and it is likely that extensional sites such as those described for the footwall did not form during deformation.

Relation of mineralized zones to lamprophyre dykes

Intrusion of the lamprophyre dykes was intimately related to Miocene development of the Moonlight Generation of structures (Cooper et al. 1987). These dykes fill extensional fractures that formed at a high angle to the N to NE trend of the Moonlight Generation folds and commonly cut across those folds. Most dykes have E or SE strikes, with some oriented NE (Fig. 2), similar to the mineralized faults of the Shotover–Macetown area (Fig. 4b,c). In addition, kink folds with axes parallel to the strike of dyke-hosting fractures commonly occur along the margins of dykes. Furthermore, dykes are commonly accompanied by ankerite veins and alteration in the host schist. Some of that alteration includes silicification and quartz veining. All of these features are identical to those of the fault-related auriferous and non-auriferous hydrothermal alteration zones of the Shotover and Macetown areas (above).

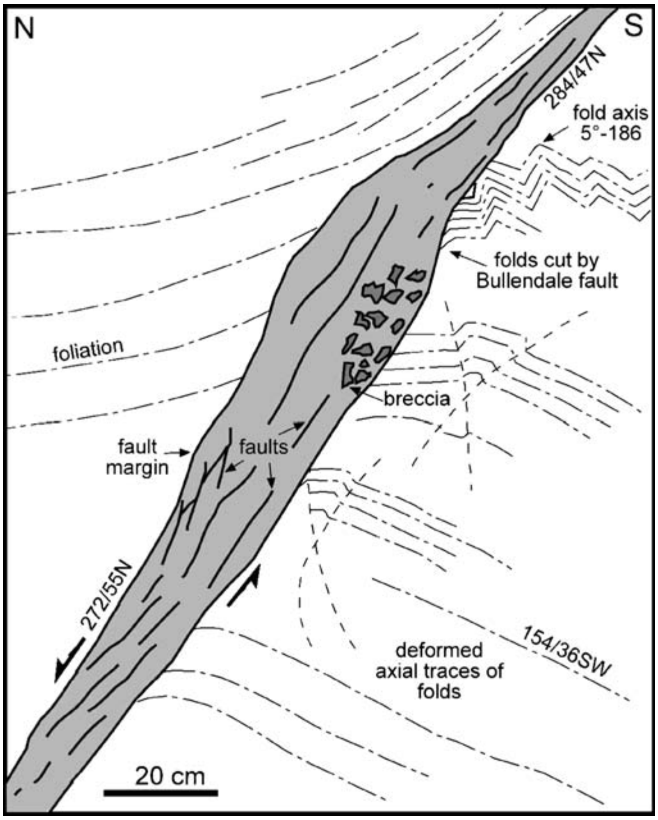

Fig. 10 Sketch showing the internal structure of a mineralized zone in the Bullendale mine underground workings (Fig. 4). The mineralized zone truncates Moonlight Generation folds in the host rock, and rotation of the schist foliation towards the fault zone indicates a normal sense of separation

There are clearly close geometrical and temporal relations between the lamprophyres and some gold emplacement structures (Figs. 2, 3). On this basis, we infer that lamprophyre dykes and gold-bearing veins were emplaced at the same time, in extensional brittle fractures formed during Moonlight Fault reversal, during and after the inception of the Alpine Fault. However, the gold and lamprophyre occurrences do not overlap spatially apart from minor gold-bearing veins immediately west of Lake Wanaka (Figs. 2, 3). The spatial separation results from the focusing of lamprophyre dykes around an igneous centre in the Haast area where carbonatites occur (Cooper 1986), whereas gold deposits were focussed in a swarm of extensional structures at the southern termination of the Shotover Antiform (above).

Despite the close structural and temporal relations between veins and dykes, there is no evidence for a direct genetic relation between gold and dykes, and there are some geochemical differences. The gold deposits are strongly silicified and veined, which results in dilution of elements that are not enriched such as major elements sodium and potassium (Fig. 12a). In contrast, fenite alteration zones at Haast are distinctly enriched in sodium and depleted in potassium (Fig. 12a; Paterson 1992). Gold-related alteration has enrichment in Sr but depletion in Ba (Fig. 12b; Craw et al. 1991), whereas fenitisation has enrichment in both Sr and Ba (Fig. 12b; Paterson 1992). Fenites are enriched in some rare earth elements, including Nb, but depleted in Rb (Fig. 12c; Cooper 1986; Paterson 1992), whereas mineralized Shotover rocks show no such changes apart from dilution effects (Fig. 12c).

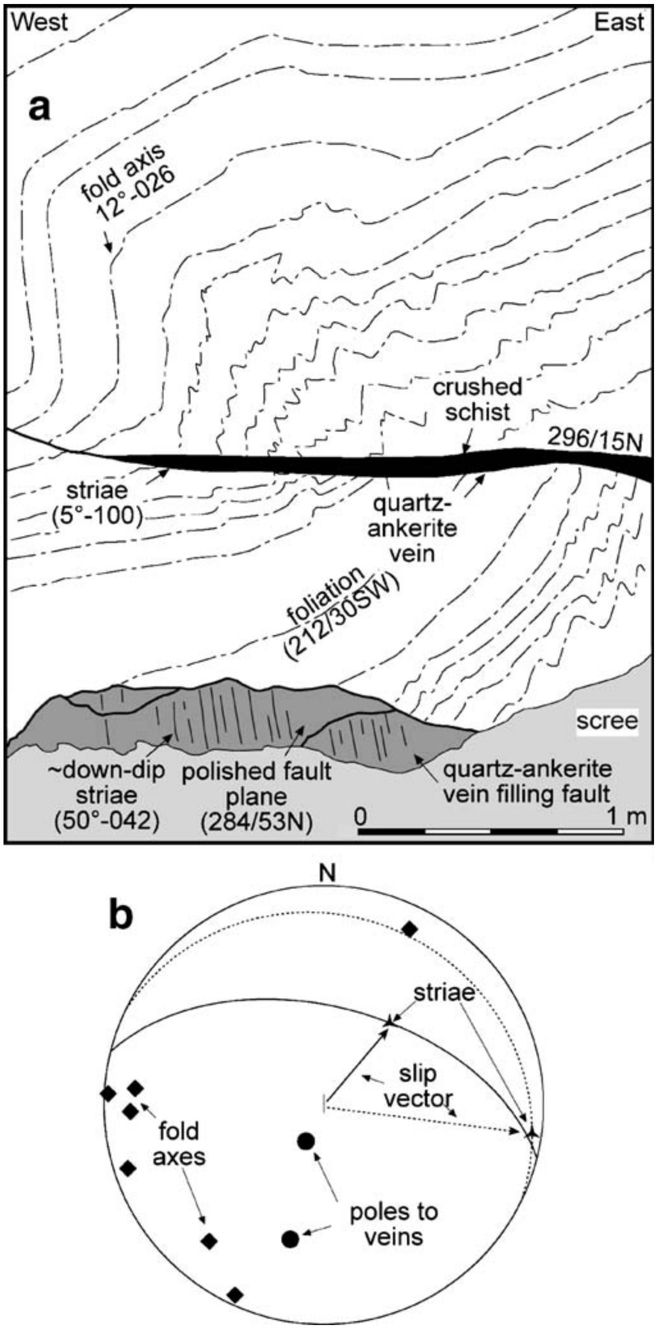

Fig. 11 Field sketch of an outcrop in a zone of ankerite/quartz alteration near Mt. Aurum (Fig. 3). **a** Low-angle quartz–ankerite vein cuts through the axial surface of a kink fold. Striae on vein surfaces indicate an easterly sense of movement. An easterly striking fault filled with quartz–ankerite vein material cuts this earlier low-angle vein. Striae and fibrous steps on the fault surface indicate a normal dip-slip sense of movement. **b** Lower hemisphere stereonet of structural elements in **a** (see text)

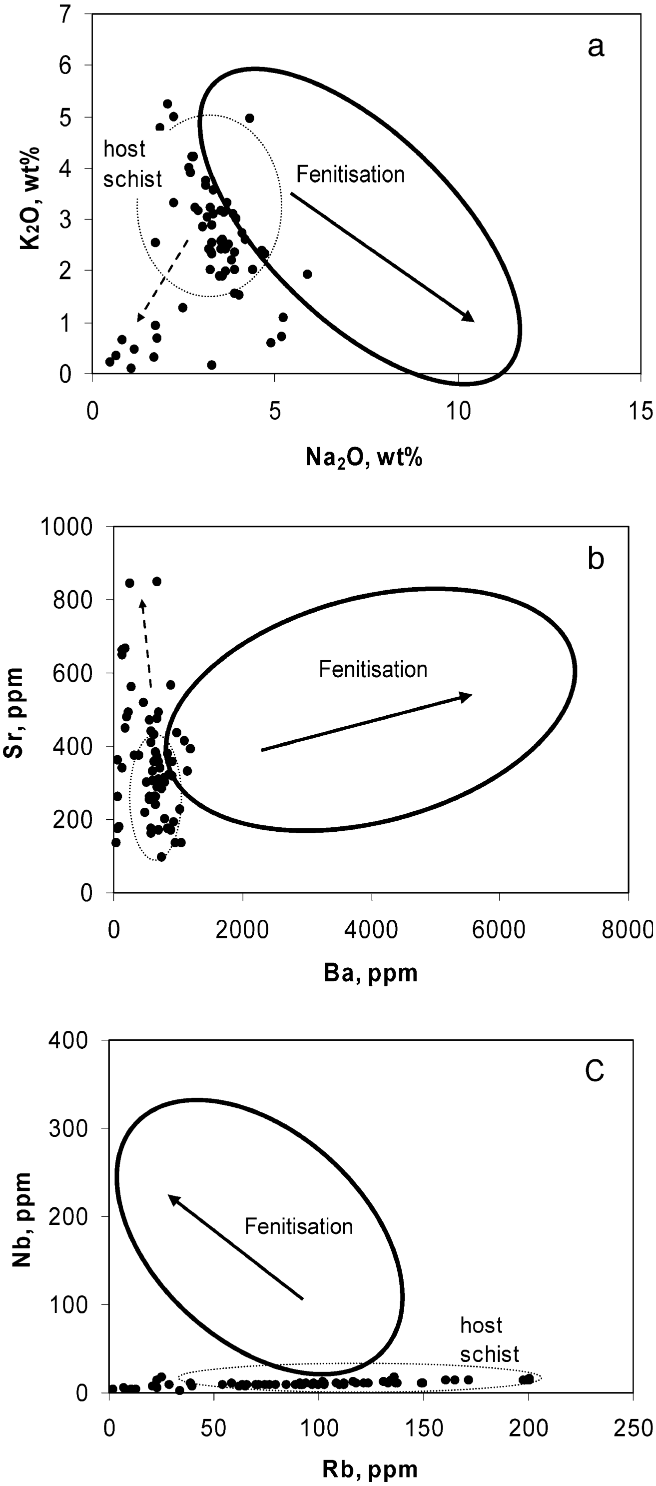

Fig. 12 Geochemical cross-plots comparing chemical effects of hydrothermal alteration at the Bullendale mine (*black dots*, this study) with fenitisation (*heavy black ellipses*, *black arrows*) associated with carbonatites in the Haast area (Fig. 1; Cooper 1986; Paterson 1992). **a**, **b** *Dashed arrows* show trends of progressive alteration at Bullendale. Host rock range is indicated with *dotted ellipses*

The stable isotopic signature of Shotover Au-related ankerite also distinguishes this alteration from carbonates associated with the carbonatites and lamprophyres from Haast (Fig. 13). The carbonatite-related data fall close to that of primary igneous carbonatite with minor oxygen shift because of interaction with the schist host (Fig. 13; Blattner and Cooper 1974). In contrast, Shotover Au-related ankerite has much higher $\delta^{18}O$ and a similar range of $\delta^{13}C$ to that of the host schist (Fig. 13; Craw et al. 1991). The isotopic differences may be a result of initial fluid compositional differences. Alternatively, the isotopic signature of Au-related ankerite may be a result of enhanced interaction of a single fluid with host schist.

The geochemical differences lead us to discount a genetic relation between lamprophyres and gold in this orogen, although some results are equivocal, and further geochemical work would be required to reach more definitive conclusions. Taylor et al. (1994), Kerrich and Wyman (1994) and Ashley et al. (1994) also discounted direct genetic links between gold and lamprophyres in other orogens.

Mineralization in the early stages of orogenesis

Mesothermal (orogenic) gold deposits are generally considered to have formed in the latter stages of orogenesis (Forde 1991; Groves et al. 2003; Goldfarb et al. 2005). This conclusion is based on the widespread observations that the deposits structurally cut across fabrics formed during orogenesis, and most of the deposits are largely unaffected by syn- to late-orogenic deformation that has affected the host rocks. Some deformed and/or metamorphosed gold deposits do occur, and these are commonly considered to represent the earliest stages of late-orogenic mineralization during initial stages of late-orogenic uplift (Cassidy and Hagemann 1999; Goldfarb et al. 2005).

In contrast, the deposits described above clearly formed in the earliest stages of evolution of the Southern Alps orogen, in the Miocene. These deposits do cut a

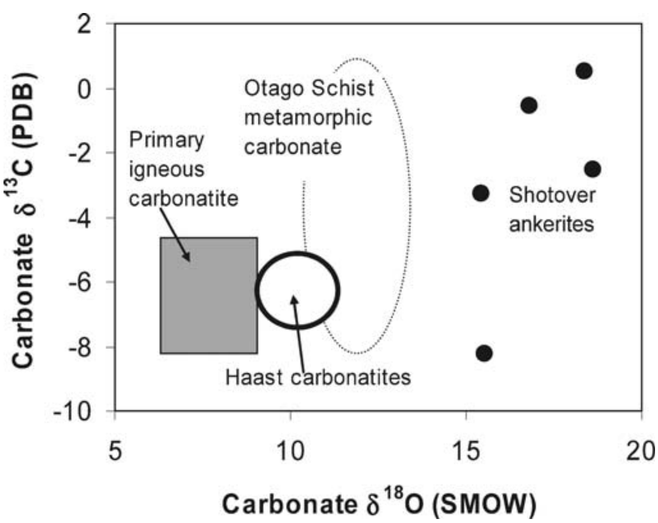

Fig. 13 Stable isotopic ranges for carbonates from host schist (*dashed ellipse*) and carbonatites (*grey filled square* and *black circle*) (after Blattner and Cooper 1974) compared with ankerites from alteration zones in the Shotover (Craw et al. 1991)

metamorphic fabric, but that fabric is a Mesozoic feature, inherited from a previous orogenic cycle. The earliest stages of mineralization described above involved infilling of extensional sites formed during Moonlight Generation folding. This folding, and reversal of the Moonlight Fault that accompanied it, represents the earliest deformational stage of the development of the Southern Alps in the Miocene. The compressive deformation that accompanied the mineralization was subsidiary to the principal tectonic process occurring at that time, the development of the Alpine Fault as a major strike-slip plate boundary (Cooper et al. 1987). However, the compressive deformation was instrumental in creating conduits and depositional sites for gold-bearing fluids and associated hydrothermal alteration.

In addition to auriferous veins subparallel to fold axial surfaces, many of the gold deposits cut across Moonlight Generation folds and fill extensional structures at a high angle to the fold trends. The lamprophyre dykes have similar cross-cutting relations to the Moonlight Generation folds. These cross-cutting structures occur throughout the area from Shotover to Haast and the Alpine Fault (Figs. 1, 2). The cross-cutting structures may be directly related to development of the compressive Moonlight Generation folds, perhaps as extensional a–c joints that commonly develop perpendicular to fold axes (McClay 1987). Mineralized mesoscopic (<metre scale) a–c joints occur in some intense Moonlight Generation fold zones (above). Alternatively, extensional faults are predicted to accompany a major strike-slip fault such as the Alpine Fault and to form at c. 60° to that major fault (Cooper et al. 1987). Hence, the cross-cutting structures may be directly related to the regional plate boundary development, as suggested by Cooper et al. (1987), rather than indirectly via a relation to the Moonlight Generation. In addition, there may have been a more local structural control on the well-defined gold-bearing belt at the southern end of a regional antiform (above). Whatever their controlling influence, it is clear that these structures provided pathways for both fluid and alkaline magmas from the middle crust and beyond at the time of initiation of the new plate boundary and the initial stages of development of the Southern Alps.

Our observations of the Shotover deposits show that gold-bearing fluids were moving through the orogen from its inception. Exposure of gold occurrences throughout the Southern Alps (Fig. 1) shows that gold-bearing fluids have continued to permeate the orogen wherever structural permeability permits (Fig. 3; Craw and Campbell 2004). The Southern Alps orogen is still young and will persist until significant changes occur to the geometry of the plate boundary. Hence, this Southern Alps example suggests that mesothermal gold mineralization can occur in the early stages of orogenic evolution, not just at the end. We suggest that early orogenic gold deposits are not recognized in ancient orogens because the deposits were progressively eroded during orogenic development, and only the latest stage of mineralization was preserved. The Shotover deposits described herein have been preserved because the principal locus of deformation in the orogen migrated northeast (Fig. 3), and the early-formed structures have not yet been overprinted at the southern end.

Conclusions

Gold mineralization and associated hydrothermal quartz-ankerite alteration occurred in localized (metre-scale) extensional structural sites associated with tight folding of fissile greenschist facies Otago Schist in the Shotover–Macetown area, southern New Zealand. The extensional sites were filled with quartz–ankerite veins and variably silicified breccias. Mineralogically and texturally similar mineralized zones fill normal faults at a high angle to the trend of the schist folds and cut across those folds. Gold is associated with pyrite and arsenopyrite that fill veins and impregnate breccia fragments. Stibnite occurs as pods within some veins and breccias, commonly in close association with the other sulphides. The extensional sites developed during regional compressional deformation of the host schist and overlying Oligocene sediments.

The hydrothermal activity and gold mineralization occurred during Miocene initiation of the Southern Alps of New Zealand along the developing Pacific–Australian plate boundary. These orogenic (mesothermal) gold deposits formed in the earliest stage of this orogenesis, which continues today. Hence, orogenic gold deposits are not formed only in the latter stages of orogenesis, as is commonly believed, but are an integral part of mountain-building processes from the inception of an orogen. The deposits described in this study are still preserved in the Southern Alps because the main locus of deformation migrated northwards in the late Cenozoic, and these early-formed deposits have not yet been structurally overprinted or uplifted and eroded. Overprinting has probably obscured early-formed deposits in ancient orogens, or early deposits have been eroded.

The fault-controlled hydrothermal mineralization and associated gold deposits have the same relative age, structural orientation and tectonic setting as a swarm of Miocene lamprophyre dykes, and some carbonatites, which cut the host schist immediately to the north of the Shotover–Macetown goldfields. Widespread ankeritic alteration, with some quartz, accompanied lamprophyre intrusion, and fenitisation has occurred adjacent to the carbonatites. The fenitisation has a distinctly different geochemical signature from the gold-related hydrothermal alteration. Emplacement of the lamprophyre intrusions and the gold-bearing veins appear to have been controlled by the same structural plumbing system in the schist host during the inception of the mountain belt. However, there does not appear to be a genetic relation between gold and lamprophyres in this orogen.

Acknowledgements This study was supported financially by the NZ Foundation for Research, Science and Technology, and the University of Otago. Permission to collect samples in a conservation area was kindly given by the Department of Conservation. Discussions with Alan Cooper, Peter Koons, Richard Norris and Rick Sibson helped us develop the ideas expressed herein. Constructive comments from James Macdonald and Anthony Harris improved the presentation.

References

Ashley PM, Cook NDJ, Hill RL, Kent AJR (1994) Shoshonitic lamprophyre dykes and their relation to mesothermal Au-Sb veins at Hillgrove, New South Wales, Australia. Lithos 32:249–272

Begbie M, Craw D (2006) Gold mineralisation in the Shotover–Macetown region, NW Otago, New Zealand. In: Christie AB, Brathwaite R (eds) Geology and exploration of New Zealand mineral deposits. AIMM Monogr 25:299–304

Bierlein FP, Crowe D (2000) Phanerozoic orogenic lode gold deposits. In: Hagemann SG, Brown PE (eds) Gold in 2000. Rev Econ Geol 13:103–140

Blattner P, Cooper AF (1974) Carbon and oxygen isotopic composition of carbonatitic dikes and metamorphic country rock of the Haast Schist terrain, New Zealand. Contrib Mineral Petrol 44:17–27

Carter RM, Norris RJ (1976) Cainozoic history of southern New Zealand: an accord between geological observations and plate tectonic predictions. Earth Planet Sci Lett 31:85–94

Cassidy KF, Hagemann SG (1999) Archean high P-T, granitoid-hosted gold mineralization at Westonia, Western Australia: I. Evidence for syn-peak metamorphic mineralization in a high grade terrain. In: Stanley CJ (ed) Mineral deposits, processes to processing. Balkema, Rotterdam, pp 1013–1016

Cooper AF (1986) A carbonatitic lamprophyre dike swarm from the Southern Alps, Otago and Westland. Cenozoic volcanism in New Zealand. R Soc N Z Bull 23:313–336

Cooper AF, Barreiro BA, Kimbrough DL, Mattinson JM (1987) Lamprophyre dike intrusion and the age of the Alpine fault, New Zealand. Geology 15:941–944

Cox SF, Wall VJ, Etheridge MA, Potter TF (1991) Deformation and metamorphic processes in the formation of mesothermal vein-hosted gold deposits: examples from the Lachlan Fold Belt in central Victoria, Australia. Ore Geol Rev 6:391–423

Craw D (1985) Structure of the schists in the Mt Aspiring region, northwestern Otago. N Z J Geol Geophys 28:55–75

Craw D (1989) Shallow-level, late-stage gold mineralisation in Sawyers Creek, Shotover valley, North West Otago, New Zealand. N Z J Geol Geophys 32:375–384

Craw D (1995) Reinterpretation of the erosion profile across the southern portion of the Southern Alps, Mt Aspiring area, Otago, New Zealand. N Z J Geol Geophys 38:501–507

Craw D (2002) Geochemistry of late metamorphic hydrothermal alteration and graphitisation of host rock, Macraes gold mine, Otago Schist, New Zealand. Chem Geol 191:257–275

Craw D (2006) Gold-bearing veins in the Southern Alps, New Zealand In: Christie AB, Brathwaite R (eds) Geology and exploration of New Zealand mineral deposits. AIMM Monogr 26:285–288

Craw D, Campbell JR (2004) Tectonic and structural setting for active mesothermal gold vein systems, Southern Alps, New Zealand. J Struct Geol 26:995–1005

Craw D, Norris RJ (1991) Metamorphogenic Au–W veins and regional tectonics: mineralisation throughout the uplift history of the Haast Schist, New Zealand. N Z J Geol Geophys 34:373–383

Craw D, Reay A, Johnstone RD (1991) Hydrothermal alteration geochemistry of Nugget gold vein system, Shotover valley, northwest Otago, New Zealand. N Z J Geol Geophys 34:419–427

Craw D, Koons PO, Horton T, Chamberlain CP (2002) Tectonically driven fluid flow and gold mineralisation in active collisional orogenic belts: comparison between New Zealand and western Himalaya. In: Labaume P, Craw D, Lespinasse M, Muchez P (eds) Tectonic processes and flow of mineralizing fluids. Tectonophysics 348:135–153

DeMets C, Gordon RG, Argus DF, Stein S (1994) Effect of recent revisions to the geomagnetic reversal time scale on estimates of current plate motions. Geophys Res Lett 21:2191–2194

Forde A (1991) The late orogenic timing of mineralization in some slate belt gold deposits, Victoria, Australia. Miner Depos 26:257–266

Goldfarb RJ, Groves DI, Gardoll S (2001) Orogenic gold and geologic time: a global synthesis. Ore Geol Rev 18:1–75

Goldfarb RJ, Baker T, Dube B, Groves DI, Hart CJ, Gosselin P (2005) Distribution, character and genesis of gold deposits in metamorphic terranes. In: Hedenquist JW, Thompson JFH, Goldfarb RJ, Richards JP (eds) Economic Geology 100th Anniversary Volume. Society of Economic Geologists, Littleton, pp 407–450

Gray DR, Foster DA (2004) $^{40}Ar/^{39}Ar$ thermochronologic constraints on deformation, metamorphism and cooling/exhumation of a Mesozoic accretionary wedge, Otago Schist, New Zealand. Tectonophysics 385:181–210

Groves DI, Goldfarb RJ, Robert F, Hart CJR (2003) Gold deposits in metamorphic belts: overview of current understanding, outstanding problems, future research, and exploration significance. Econ Geol 98:1–29

Jackson J, Norris RJ, Youngson JH (1996) The structural evolution of active fault and fold systems in Central Otago, New Zealand: evidence revealed by drainage patterns. J Struct Geol 18:217–234

Kerrich R, Wyman DA (1994) The mesothermal gold lamprophyre association: significance for an accretionary geodynamic setting, supercontinent cycles, and metallogenic processes. Min Pet 51:147–172

McClay K (1987) The mapping of geological structures. Geological Society of London Handbook. Wiley, New York, p 161

Nesbitt BE, Murowchick JB, Muehlenbachs K (1986) Dual origins of lode gold deposits in the Canadian Cordillera. Geology 14:506–509

Norris RJ, Craw D (1987) Aspiring Terrane: an oceanic assemblage from New Zealand and its implications for terrane accretion in the southwest Pacific. Geodynamics 19:169–177

Norris RJ, Koons PO, Cooper AF (1990) The obliquely convergent plate boundary in the South Island of New Zealand: implications for ancient collision zones. J Struct Geol 12:715–726

Paterson L (1992) A study of carbonatites and associated fenirisation at Haast River, southwestern New Zealand. Unpublished Ph.D. thesis, University of Otago Library, Dunedin

Rock NMS, Groves DI, Perring CS, Golding SD (1989) Gold, lamprophyres, and porphyries: what does their association mean? In: Keays RR, Ramsay RH, Groves DI (eds) The geology of gold deposits. Econ Geol Monogr 6:609–625

Sibson RH, Scott J (1998) Stress/fault controls on the containment and release of overpressured fluids: examples from gold–quartz vein systems in Juneau, Alaska; Victoria, Australia; and Otago, New Zealand. Ore Geol Rev 13:293–306

Sibson RH, Robert F, Poulsen KH (1988) High-angle reverse faults, fluid-pressure cycling, and mesothermal gold–quartz deposits. Geology 16:551–555

Simpson GD, Cooper AF, Norris RJ (1994) Late Quaternary evolution of the Alpine Fault Zone at Paringa, South Westland, New Zealand. N Z J Geol Geophys 37:49–58

Taylor WR, Rock NMS, Groves DI, Perring CS, Golding SD (1994) Geochemistry of Archean shoshonitic lamprophyres from the Yilgarn Block, Western Australia: Au abundance and association with gold mineralization. Appl Geochem 9:197–222

Teagle DAH, Norris RJ, Craw D (1990) Structural controls on gold-bearing quartz mineralization in a duplex thrust system, Hyde-Macraes Shear Zone, Otago Schist, New Zealand. Econ Geol 85:1711–1719

Teagle DAH, Hall CM, Cox SC, Craw D (1998) Ar/Ar dating and uplift rate of hydrothermal minerals in the Southern Alps, New Zealand. In: Arehart GB, Hulston JR (eds) Proceedings, 9th International Symposium on Water–Rock Interaction. Balkema, Rotterdam, pp 801–804

Turnbull IM (2000) Geology of the Wakatipu area. Institute of Geological & Nuclear Sciences 1:250 000 geological map 18. 1 sheet + 72p. Institute of Geological & Nuclear Sciences, Lower Hutt

Turnbull IM, Barry JM, Carter RM, Norris RJ (1975) The Bobs Cove beds and their relationship to the Moonlight Fault Zone. J R Soc N Z 5:355–394

Wellman H (1979) An uplift map for the South Island of New Zealand, and a model for uplift of the Southern Alps. In: Walcott RI, Cresswell MM (eds) The origin of the Southern Alps. R S N Z Bull 18:13–20

Williams GJ (1974) Economic geology of New Zealand. AIMM Monogr 4

Witt WK, Vanderhor F (1998) Diversity within a unified model for Archean gold mineralization in the Yilgarn Craton of Western Australia: an overview of the late-orogenic structurally controlled gold deposits. Ore Geol Rev 13:29–64